

[⁶⁸Ga]Ga-PSMA-11 PET/CT improves tumor detection and impacts management in patients with hepatocellular carcinoma

Short running title

PSMA PET for HCC

Authors

Nader Hirmas¹, Catherine Leyh², Miriam Sraieb¹, Francesco Barbato¹, Benedikt M. Schaarschmidt³, Lale Umutlu³, Michael Nader¹, Heiner Wedemeyer², Justin Ferdinandus¹, Christoph Rischpler¹, Ken Herrmann¹, Pedro Fragoso Costa¹, Christian M. Lange², Manuel Weber^{1*}, Wolfgang P. Fendler^{1*}

Affiliations

¹ Department of Nuclear Medicine, University of Duisburg-Essen and German Cancer Consortium (DKTK)-University Hospital Essen, Essen, Germany

² Department of Gastroenterology and Hepatology, University Hospital Essen, University Duisburg-Essen, Essen, Germany

³ Institute of Diagnostic and Interventional Radiology and Neuroradiology; University Hospital Essen, University Duisburg-Essen, Essen, Germany

*contributed equally

Corresponding author

Name: Wolfgang P. Fendler, MD

Address: Hufelandstraße 55, 45147 Essen, Germany

Tel.: +49 201 723 2032

Fax: +49 201 723 5658

E-mail: wolfgang.fendler@uk-essen.de

First author

Name: Nader Hirmas, MD

Position: Doctoral candidate

Address: Hufelandstraße 55, 45147 Essen, Germany

Tel.: +49 201 723 2032

Fax: +49 201 723 5658

E-mail: nader.hirmas@stud.uni-due.de

Word count

5,258 words.

Financial support

None.

ABSTRACT

Rationale: Hepatocellular carcinoma (HCC) is the sixth most prevalent cancer and the third most frequent cause of cancer-related death. A growing number of local and systemic therapies are available, and accurate staging is critical for management decisions. We assessed the impact of neovasculature imaging by ^{68}Ga -Ga-PSMA-11 PET/CT on disease staging, prognostic groups and management of patients with HCC compared to staging with computed tomography (CT).

Methods: Forty patients who received imaging with ^{68}Ga -Ga-PSMA-11 PET/CT for HCC staging between September 2018 and September 2019 were retrospectively included. Management pre- and post-PET scan was assessed by standardized surveys. Presence of HCC was evaluated by three blinded readers on a per-patient and per-region basis for PET/CT (PET criteria) and multi-phase contrast-enhanced CT (CT criteria) in separate sessions. Lesions were validated by follow-up imaging or histopathology, and progression-free survival (PFS) was recorded. Endpoints were detection rate and positive predictive value (PPV) for ^{68}Ga -Ga-PSMA-11 PET vs. CT, inter-reader reproducibility, and changes in stage, prognostic groups and management plans.

Results: Median age was 65 years (range, 37-81), median Child-Pugh score was 5 (range, 5-9). Most patients were treatment naïve (27 of 40, 67.5%). The sensitivity of PET vs. CT to identify liver lesions for patients with lesion validation was 31/32 (97%) for both modalities, while it was 6/6 (100%) vs. 4/6 (67%) for extra-hepatic lesions. PET and CT each had a PPV of 100% at the liver level. PET vs. CT stage was congruent in 30/40 (75%) patients; upstaging was seen in 8/40 patients (20%), while 2/40 (5%) had downstaging by PET. Intended management changed in 19/40 patients (47.5%); 9/19 of

these patients were found to have detectable distant metastases (47.4%) and assigned stage 4 disease, the majority of whom were shifted to systemic therapy (8 of 9, 89%). Two patients underwent ^{177}Lu -Lu-PSMA-617 radioligand therapy. Median PFS was 5.2 months for the entire cohort; 5.3 months for PET M0, and 4.7 months for PET M1 patients, respectively.

Conclusion: ^{68}Ga -Ga-PSMA-11 PET demonstrated higher accuracy than CT in the detection of HCC metastases and was associated with management change in about half of the patient cohort.

Keywords

Hepatocellular carcinoma; PSMA; PET; staging; theranostic

INTRODUCTION

Hepatocellular carcinoma (HCC) is the sixth most prevalent cancer and the third most frequent cause of cancer-related death worldwide (1).

Early-stage HCC is often treated with surgical resection, transplantation or ablation, while systemic therapy, trans-arterial chemoembolization (TACE) and radioembolization (also known as selective internal radiation therapy (SIRT)) are reserved for intermediate to advanced HCC, with SIRT being most often used after progression under sorafenib (2,3). The treatment landscape for HCC changed considerably with the availability of life-prolonging systemic therapy. Despite recent therapy approvals, patient survival remains short, and accurate staging is critically needed to early identify candidates for the various local and systemic therapies. The European Society for Medical Oncology guidelines recommend computed tomography (CT), magnetic resonance imaging (MRI) or ultrasound for diagnosis of HCC in patients with cirrhosis (4). However, small HCC lesions may be hard to detect, especially with concomitant cirrhosis.

⁶⁸Ga-Ga-PSMA-11 is a novel positron emission tomography (PET) tracer that has been developed for imaging patients with prostate cancer (5,6). PSMA was also found to be expressed on the neovasculature of other tumor entities (7,8), with immunohistochemistry revealing PSMA expression on HCC neovasculature and canalicular membranes, with significantly increased uptake in hepatic and extrahepatic disease (9,10). A recent prospective study on 15 patients with HCC reported improved lesion detection with ⁶⁸Ga-Ga-PSMA-11 PET/CT compared to conventional imaging and a subsequent impact on treatment strategies (11).

In light of increasing local and systemic treatment options, ^{68}Ga -Ga-PSMA-11 PET/CT may demonstrate value for staging and management of patients with initial HCC. In this study, we aim to assess the accuracy of ^{68}Ga -Ga-PSMA-11 PET/CT along with inter-reader agreement and impact on staging, management and prognostic groups in patients with initial HCC.

MATERIALS AND METHODS

Study Design and Participants

Patients undergoing ^{68}Ga -Ga-PSMA-11 PET/CT for HCC between September 2018 and September 2019 at the Essen University Hospital were retrospectively included in the study. The primary endpoint was detection rate and positive predictive value (PPV) for ^{68}Ga -Ga-PSMA-11 PET vs. CT. Secondary endpoints were inter-reader reproducibility, and changes in stage, prognostic group and management plans. All patients gave written consent to undergo clinical ^{68}Ga -Ga-PSMA-11 PET/CT. The retrospective study was approved by the ethics committee at the University Duisburg-Essen (approval no. 19-8892-BO) and need for consent was waived. Anonymized study data were collected retrospectively and managed using the Research Electronic Data Capture (REDCap) electronic data capture tools hosted at the University Hospital Essen (12,13). Patients' records were accessed to retrieve demographic and clinical data, pathology and lab investigations, as well as imaging studies performed prior to or after ^{68}Ga -Ga-PSMA-11 PET/CT.

Imaging procedures

^{68}Ga -Ga-PSMA-11 (Glu-NH-CO-NH-Lys-(Ahx)-[^{68}Ga (HBED-CC)]) was labeled in accordance with the joint European Association of Nuclear Medicine (EANM) and Society of Nuclear Medicine and Molecular Imaging (SNMMI) procedure guideline (14). PET was acquired in accordance with the international guidelines as part of a PET/CT and with a field of view from the skull base to the mid-thigh. Patients received a median of 112.5 MBq (range, 79-344 MBq) of ^{68}Ga -Ga-PSMA-11. Image acquisition was started after a median of 78 minutes post injection (range, 50 – 135; interquartile range 31.5).

All of the 40 examinations were performed with radiographic contrast enhancement in arterial and portal venous phase, contrast enhanced CT was performed prior to PET acquisition. Images were acquired using Siemens 128mCT in 29/40 cases (72.5%) and Siemens mCT VISION in 11/40 cases (27.5%), both devices are cross-calibrated based on EARL accreditation standards. PET images were reconstructed by ordered subset expectation maximization based algorithms. Data from CT scans were used for attenuation correction and anatomical correlation.

Image Interpretation

Three nuclear medicine physicians (M.W., M.S., F.B.) blinded to all clinical and imaging data interpreted the images separately: first, the attenuation-corrected ^{68}Ga -Ga-PSMA-11 PET and CT images using PET criteria, and two weeks later, CT images only using CT criteria. OsiriX MD (Pixmeo SARL, Switzerland) was used for the readings.

The presence of HCC lesions was recorded separately for ^{68}Ga -Ga-PSMA-11 PET and CT across five regions (positive/negative): liver segments, abdominal and extra-abdominal lymph nodes, peritoneal/visceral lesions and bone lesions.

For PET interpretation only, a 4-point scale was used to visually rate focal radioligand uptake (from 0-3) (15,16) with corresponding CT scans used for anatomical correlation. Focal uptake was considered positive with score ≥ 1 (extrahepatic lesions) or score ≥ 2 (hepatic lesions). Differentiating between HCC lesions vs. dysplastic nodules on CT scan (or MRI in case of follow-up imaging) followed the criteria outlined in supplemental table 1 (17,18).

Readers recorded SUV_{max} for lesions with the highest uptake and diameter of largest lesions (short axis for lymph nodes, long axis for all other lesions) at a given region. Readers determined the TNM staging separately for ^{68}Ga -Ga-PSMA-11 PET and CT in accordance with American Joint Committee on Cancer (AJCC) criteria, 8th edition (19).

Consensus (positive vs. negative) was determined by a statistic majority vote among the three readers, with average values taken for quantitative values (SUV_{max} and lesion size). Consensus findings for the ^{68}Ga -Ga-PSMA-11 PET and CT scans for each patient were compared to determine concordance.

Lesion Validation and Change in Management

Patient files were reviewed for correlative and follow-up information acquired during routine clinical follow-up. CT, MRI, bone scans and ^{68}Ga -Ga-PSMA-11 PET scans performed as pre-imaging and on follow-up were included in this analysis.

The best valuable comparator with the following priority order (highest to lowest) was used to assign true or false positivity and negativity to detected lesions: histopathology from biopsies or surgical excision took priority over imaging validation; lesions were also confirmed by presence on the initial and follow-up scans; as well as their change in size, disappearance or appearance on follow-up imaging during treatment, using mRECIST criteria (20). Any lesion that could not be verified based on those criteria was excluded from the accuracy analyses. The local investigators interpreted the composite reference standard after reviewing follow-up information.

Management plan before PET was local therapy, including SIRT, radiofrequency ablation (RFA) or TACE as documented by the interdisciplinary tumor board. Implemented management after PET was recorded by the referring physician using a standardized survey.

Statistical Analysis

Descriptive statistics were calculated. Inter-observer agreement was determined by Fleiss' κ and interpreted by the criteria of Landis and Koch (21). PPV, negative predictive value (NPV), sensitivity and specificity on a per-patient and per-region-basis of ^{68}Ga -Ga-PSMA-11 PET for detection of tumor location confirmed by histopathology/biopsy, clinical and conventional imaging follow-up were calculated via standard 2 x 2 tables. PET progression-free survival (PFS) was calculated from the date of ^{68}Ga -Ga-PSMA-11 PET scan until progression or death/last follow-up. κ analysis was performed using R statistics (version 3.4.1).

RESULTS

Patient Characteristics

Forty patients were included; patient characteristics are outlined in table 1. The median age was 65 years (range, 37-81). Twenty patients (50%) had histopathological confirmation of HCC; the other half had imaging findings consistent with HCC. Liver cirrhosis was present in 28/40 patients (70%). The most frequent underlying liver disease was chronic hepatitis B or C in 18/40 patients (45%). In addition, portal vein thrombosis or invasion was seen in 9/40 patients (22.5%). Eleven patients (27.5%) had ascites. Twenty-seven patients (67.5%) did not receive treatment prior to their ⁶⁸Ga-Ga-PSMA-11 PET scan.

Detection Accuracy and Lesion Validation

In total, 142 lesions from 36 patients were validated as true positive, false positive or false negative at the levels of hepatic segments (1 through 8) and extra-hepatic metastases. Lesions from eight patients (20%) were validated by histopathology, 26/40 (65%) by baseline and follow-up imaging correlation, and 10/40 (25%) by baseline imaging correlation only. All patients with histopathologic verification had follow-up imaging performed.

⁶⁸Ga-Ga-PSMA-11 PET versus CT accuracy for the liver lobes as well as distant metastases is reported in table 2. Consensus interpretation on a whole liver level for the entire cohort as well as for patients with cirrhosis (n=28/40, 70%) resulted in an accuracy of 97% for both ⁶⁸Ga-Ga-PSMA-11 PET and CT (sensitivity of 97%, specificity and PPV

of 100%, and NPV of 80%). Liver segment level data for detection rate and accuracy are given in supplemental table 2.

⁶⁸Ga-Ga-PSMA-11 PET vs. CT detected 13 versus 9 distant metastatic lesions in 11 versus 8 patients, respectively (table 3). Extrahepatic lesions were validated in 6 patients upon further follow-up: sensitivity for ⁶⁸Ga-Ga-PSMA-11 PET vs. CT was 100% vs. 67%, respectively, and the NPV was 100% vs. 93%, respectively (table 2).

Of the cases with congruence in ⁶⁸Ga-Ga-PSMA-11 PET and CT, one patient had disseminated bone metastases on pre-imaging that were confirmed on ⁶⁸Ga-Ga-PSMA-11 PET and CT (see supplemental figure 1); another patient had mediastinal lymph node metastases on ⁶⁸Ga-Ga-PSMA-11 PET and CT that were subsequently verified as positive by histopathology following lymph node resection (see supplemental figure 2); and a third patient had pathological lymph nodes in the cardiophrenic angle that were confirmed on follow-up scans (see supplemental figure 3).

Among the cases where ⁶⁸Ga-Ga-PSMA-11 PET outperformed CT, one patient had positive PSMA uptake in the right femur on ⁶⁸Ga-Ga-PSMA-11 PET that was missed on CT scan (see supplemental figure 4), and follow-up CT scans for that patient confirmed development of a osseous lesion; and a patient with positive PSMA uptake in the right 4th rib seen on ⁶⁸Ga-Ga-PSMA-11 PET but not on CT (see supplemental figure 5), with subsequent scans confirming resolution of the lesion following local treatment to the metastatic spot. The third patient had metastatic lesions in mediastinal lymph nodes and lumbar vertebra that were not deemed pathological on CT (see supplemental figures 6-I and 6-II) and was offered systemic treatment as a result. In the remaining patients with lesion validation, distant metastases were ruled out by both ⁶⁸Ga-Ga-PSMA-11 PET and

CT and were subsequently confirmed as negative on follow-up imaging.

Inter-Observer Agreement

According to Fleiss' κ , agreement among the three independent readers for PET vs. CT at the liver level was 0.43 [0.25-0.61] vs. 0.56 [0.38-0.74], respectively, indicating a “moderate” agreement according the Landis and Koch criteria. At the extrahepatic level (lymph nodes and osseous metastases), agreement for PET vs. CT was 0.83 [0.65-1.01] vs. 0.75 [0.56-0.93], respectively. This corresponds to “almost perfect agreement” for PET and “substantial” agreement for CT, according to the same criteria.

Staging Concordance and Migration

Comparison of staging between ^{68}Ga -Ga-PSMA-11 PET and CT is shown in tables 3 and 4. Concordance between ^{68}Ga -Ga-PSMA-11 PET and CT findings was seen in 30/40 patients (75%), while 8/40 patients (20%) experienced upstaging and 2/40 (5%) had downstaging by ^{68}Ga -Ga-PSMA-11 PET (supplemental table 3).

With regards to upstaged patients, 1 patient (2.5%) with no disease on CT was upstaged to post-PET stage 2. In this patient, a single lesion in liver segment 5 was found by ^{68}Ga -Ga-PSMA-11 PET and missed by CT, confirmed by histopathology (see supplemental figure 7). In addition, 6/40 patients (15%) with CT stage 2 were upstaged to post-PET stage 3 (n=4, 10%) and stage 4 (n=2, 5%); and 1 patient (2.5%) with CT stage 3 was upstaged to post-PET stage 4.

In total, there were 3/40 patients (7.5%) in whom ⁶⁸Ga-Ga-PSMA-11 PET detected distant disease that was not detected by CT. Cases are detailed previously and in supplemental figures 4, 5 and 7.

Downstaging by ⁶⁸Ga-Ga-PSMA-11 PET occurred in 2 patients: one had CT stage 2 (lesion diameter 3.4cm), but ⁶⁸Ga-Ga-PSMA-11 PET did not detect any hepatic disease. Follow-up MRI showed a lesion in segment V (diameter 2.9cm); hence, the ⁶⁸Ga-Ga-PSMA-11 PET result was deemed false negative. The other patient had a CT stage 3B (T4N0M0) but a PET stage 3A (T3N0M0), with no implications on management in this case.

A summary of concordant and discordant staging between ⁶⁸Ga-Ga-PSMA-11 PET and CT is shown in table 4. Mean lesion sizes on CT and mean SUV_{max} values on ⁶⁸Ga-Ga-PSMA-11 in different stages are summarized in supplemental table 4.

Management Follow-Up

Figure 1 illustrates changes in management after ⁶⁸Ga-Ga-PSMA-11 PET for different stage groups. Overall, pre- to post-PET/CT treatment plans changed in 19/40 patients (47.5%).

⁶⁸Ga-Ga-PSMA-11 PET detected no correlate of disease in 4/40 patients (10%). Among these, 1/4 patient (25%) experienced change in management, i.e. switch from SIRT to TACE. This was based on the original unblinded imaging report which had reported tumor foci in the liver; such findings were not reported in the consensus readings by the blinded readers and were thus considered negative.

⁶⁸Ga-Ga-PSMA-11 PET detected stage 2 disease in 5/40 patients (12.5%). Among these, 2/5 patients (40%) experienced change in management as follows: one was shifted from SIRT to systemic therapy, and the other patient was shifted to TACE from active surveillance.

Twenty patients (50%) were classified as stage 3 by ⁶⁸Ga-Ga-PSMA-11 PET, 7/20 of whom (35%) had a shift in management as follows: 6 were switched to systemic therapy due to evident portal vein and/or mesenteric vein thrombosis (n=3), proven high risk for hepatopulmonary shunt (n=1), or being deemed not suitable for SIRT treatment (n=2); the remaining patient was switched to best supportive care.

Eleven patients (27.5%) were classified as stage 4 by ⁶⁸Ga-Ga-PSMA-11 PET. The highest rate of change in management occurred in patients with stage 4B, recorded in 9 out of 11 (82%), 8/9 of whom (89%) were shifted to systemic therapy upon detection of distant metastases on ⁶⁸Ga-Ga-PSMA-11 PET scan, and TACE was performed in the remaining patient (see supplemental figure 5). Details of management changes pre- and post-⁶⁸Ga-Ga-PSMA-11 PET are highlighted in supplemental table 5.

Two patients had liver lesions with high uptake on ⁶⁸Ga-Ga-PSMA-11 PET; those patients had no other local or systemic treatment options, and they were deemed eligible for and proceeded with ¹⁷⁷Lu-Lu-PSMA-617 radioligand therapy (RLT). However, as revealed by intra-therapeutic SPECT/CT based dosimetry, the tumor radiation dose by RLT was at least ten-fold lower than typically achieved by one cycle of external beam radiation therapy for HCC, and as such, this treatment modality was not as effective as anticipated. RLT was discontinued after one cycle for both patients. RLT and dosimetry findings are summarized in supplemental figures 8 and 9.

Progression-Free Survival Outcomes

Median observation period was 8.3 months (range, 0.2 to 18.1) from ⁶⁸Ga-Ga-PSMA-11 PET/CT. Patients with observation periods of less than 6 months were either deceased (N=9/40, 22.5%) or lost to follow-up (N=4/40, 10%). During the observation period, disease progression after initial ⁶⁸Ga-Ga-PSMA-11 PET was noted for 26/40 patients (65%) as follows: 13/40 by follow-up imaging (32.5%) and 13/40 by death (32.5%). For the remaining patients, 4/40 (10%) were lost to follow-up, and 10/40 (25%) are still on regular follow-up at our institution.

Median PFS was 5.2 months. Patients with PET M0 versus M1 disease had a median PFS of 5.3 months vs. 4.7, respectively ($p=0.865$).

DISCUSSION

We compared ⁶⁸Ga-Ga-PSMA-11 PET and CT accuracy for HCC lesion detection and assessed PET impact on management and prognostic groups. Our results demonstrate comparable accuracy of ⁶⁸Ga-Ga-PSMA-11 PET and CT for staging at the liver level, with superior performance for ⁶⁸Ga-Ga-PSMA-11 PET at the extrahepatic level with “almost perfect agreement” among the independent readers. PET/CT accuracy was associated with management change, particularly in patients with advanced disease, leading to a shift towards systemic therapy. PET detection of extra hepatic disease was not associated with shorter PFS.

HCC treatment decisions depend on a multidisciplinary approach that take into account several factors including size, extent of tumor burden, and functional status of

the liver (22). For intermediate- and advanced-stage disease, standard of care includes RFA, TACE, radioembolization or systemic therapy, while patients with end-stage disease often receive palliative care only (2,23-25). The majority of patients with HCC present with advanced disease and poor prognosis (26,27). Imaging is critical to accurately assess local and distant disease extent at baseline and follow-up, therefore refining identification of candidates for systemic treatment.

Currently, international treatment guidelines place sorafenib as the standard first-line systemic therapy for patients with advanced HCC or earlier stage tumors progressing upon or unsuitable for loco-regional therapies (2,23-25). Current FDA approved first-line treatments for advanced/progressive HCC are sorafenib or lenvatinib, which are associated with prolonged survival in patients with advanced tumors (28-30). New options include bevacizumab in combination with atezolizumab as first-line therapy, as well as regorafenib, cabozantinib, and ramucirumab, in addition to immunotherapy agents like nivolumab and pembrolizumab as second-line therapies (31). PSMA-directed systemic treatments such as mipsagargin (G-202) have also been recently studied, with preliminary results showing prolonged disease stabilization in patients with HCC who progressed on or after sorafenib or were intolerant of it (32).

⁶⁸Ga-Ga-PSMA-11 PET identified distant disease earlier and led to change towards systemic treatment in our study. In this non-randomized observational setting, PFS was not significantly different for PET M0 versus M1 patients. PET may contribute to improved outcome of metastatic HCC through earlier identification of candidates for systemic therapy. However, assessment in a prospective trial is needed, as our retrospective observation is limited to the assessment of stage migration with reported

impact on management.

A systematic review and meta-analysis summarized the existing evidence on multiphase CT versus MRI accuracy for the diagnosis of HCC in patients with underlying cirrhosis (33). Pooled analysis of the 19 studies comparing both modalities showed significantly higher sensitivity (0.82 vs. 0.66) and lower negative likelihood ratio (0.20 vs. 0.37) for MRI over CT. In our study, ⁶⁸Ga-Ga-PSMA-11 PET and CT demonstrated similar detection rate and accuracy at the liver level for both, the entire cohort, as well as the subset of patients with cirrhosis. Thus, PET will not replace MRI for accurate liver staging. It is also worth noting that underlying cirrhosis did not affect lesion PSMA uptake (median SUV_{max} for patients with cirrhosis and for those without cirrhosis was 14.1).

HCC diagnosis is more often based on imaging rather than biopsy (2); therefore, histopathologic information pertaining to tumor grade and aggressiveness is often missing. ¹⁸F-labelled choline derivatives, like ¹⁸F-FECH and ¹⁸F-FCH, have demonstrated value in identifying differentiated, less aggressive HCC, while ¹⁸F-FDG is useful in identifying less differentiated, more aggressive tumor forms (34). In one study, dual-tracer PET/CT (using ¹⁸F-FCH and ¹⁸F-FDG) enabled stage upgrading in 11% and treatment modification in 14% of patients (35). With documented expression of PSMA in tumor neovasculature and canalicular membranes of HCC, ⁶⁸Ga-Ga-PSMA-11 PET is a new diagnostic modality; however, correlation with tumor differentiation and aggressiveness requires further assessment.

Our study is limited by its retrospective design as well as the small number of patients included. Histopathology was available in a small group of patients only as tissue sampling is not routinely performed, and biopsy of extrahepatic lesions is difficult due to

small size or remote location. Thus, majority of lesion follow-up was based on correlative or follow-up imaging with known intrinsic limitations. In addition, MRI or PET/MRI was not systematically performed for comparison in the included patients. Finally, 18/40 (45%) of patients had an uptake time outside the EANM/SNMMI recommended range of 50 to 100 minutes (14), which may have impacted image interpretation.

CONCLUSION

In summary, using blinded reads and independent lesion validation, we establish accuracy of ⁶⁸Ga-Ga-PSMA-11 PET for HCC staging, which was comparable for hepatic and more accurate for extra-hepatic disease detection when compared to CT. ⁶⁸Ga-Ga-PSMA-11 PET induced stage migration by detection of distant metastases in 11/40 patients (27.5%), which was associated with a shift from local to systemic therapy in 8/11 (73%) of these patients. ⁶⁸Ga-Ga-PSMA-11 PET may prove valuable for early identification of candidates for systemic therapy.

DISCLOSURES

Conflicts of Interest

Ken Herrmann reports personal fees from Bayer, SIRTEX, Adacap, Curium, Endocyte, IPSEN, Siemens Healthineers, GE Healthcare, Amgen, Novartis and ymabs, as well as personal and other fees from Sofie Biosciences, non-financial support from ABX, and grants and personal fees from BTG, all of which are outside of the submitted work. Christian M. Lange has received speaker and consultancy fees from Abbvie, MSD, Roche, Eisai, Behring, Falk, Novartis and Norgine, all of which are outside of the

submitted work. Manuel Weber is on the Speakers Bureau for Boston Scientific. Wolfgang P. Fendler is a consultant for Endocyte and BTG, and he received personal fees from RadioMedix, Bayer and Parexel as well as financial support from Mercator Research Center Ruhr (MERCUR, An-2019-0001), IFORES (D/107-81260, D/107-30240), Doktor Robert Pflieger-Stiftung, and Wiedenfeld-Stiftung/Stiftung Krebsforschung Duisburg, all of which are outside of the submitted work. No other potential conflicts of interest relevant to this article exist.

Funding/Support

Nader Hirmas was financially supported by the German Academic Exchange Service (Deutscher Akademischer Austauschdienst (DAAD)) to pursue his doctoral studies, part of which included this research project.

KEY POINTS

QUESTION: Does ^{68}Ga -Ga-PSMA-11 PET/CT improve tumor detection and impact clinical management of patients with hepatocellular carcinoma?

PERTINENT FINDINGS: This is a retrospective study assessing the impact of ^{68}Ga -Ga-PSMA-11 PET/CT imaging on disease staging, prognostic groups and management of patients with HCC compared to staging with CT. Staging accuracy for ^{68}Ga -Ga-PSMA-11 PET was comparable for hepatic and more accurate for extra-hepatic staging when compared to CT, inducing stage migration by detection of distant metastases in 11/40 patients (27.5%), with a shift from local to systemic therapy in 8/11 (73%) of these patients. ^{68}Ga -Ga-PSMA-11 PET may prove valuable for early identification of candidates for systemic therapy.

IMPLICATIONS FOR PATIENT CARE: ^{68}Ga -Ga-PSMA-11 PET demonstrated higher accuracy than CT in the detection of HCC metastases and was associated with management change in about half of the patient cohort.

REFERENCES

1. Forner A, Llovet JM, Bruix J. Hepatocellular carcinoma. *Lancet*. 2012;379:1245-1255.
2. Bruix J, Sherman M. Management of hepatocellular carcinoma: an update. *Hepatology*. 2011;53:1020-1022.
3. Lencioni R, Chen XP, Dagher L, Venook AP. Treatment of intermediate/advanced hepatocellular carcinoma in the clinic: how can outcomes be improved? *Oncologist*. 2010;15 Suppl 4:42-52.
4. Vogel A, Cervantes A, Chau I, et al. Hepatocellular carcinoma: ESMO clinical practice guidelines for diagnosis, treatment and follow-up. *Ann Oncol*. 2018;29:iv238-iv255.
5. Perera M, Papa N, Roberts M, et al. Gallium-68 prostate-specific membrane antigen positron emission tomography in advanced prostate cancer—updated diagnostic utility, sensitivity, specificity, and distribution of prostate-specific membrane antigen-avid lesions: a systematic review and meta-analysis. *Eur Urol*. 2020;77:403-417.
6. Perera M, Papa N, Christidis D, et al. Sensitivity, specificity, and predictors of positive (68)Ga-prostate-specific membrane antigen positron emission tomography in advanced prostate cancer: a systematic review and meta-analysis. *Eur Urol*. 2016;70:926-937.
7. Chang SS, O'Keefe DS, Bacich DJ, Reuter VE, Heston WDW, Gaudin PB. Prostate-specific membrane antigen is produced in tumor-associated neovasculature. *Clin Cancer Res*. 1999;5:2674-2681.
8. Chang SS, Reuter VE, Heston WD, Bander NH, Grauer LS, Gaudin PB. Five different anti-prostate-specific membrane antigen (PSMA) antibodies confirm PSMA expression in tumor-associated neovasculature. *Cancer Res*. 1999;59:3192-3198.
9. Kesler M, Levine C, Hershkovitz D, et al. (68)Ga-PSMA is a novel PET-CT tracer for imaging of hepatocellular carcinoma: A prospective pilot study. *J Nucl Med*. 2019;60:185-191.
10. Tolkach Y, Goltz D, Kremer A, et al. Prostate-specific membrane antigen expression in hepatocellular carcinoma: potential use for prognosis and diagnostic imaging. *Oncotarget*. 2019;10:4149-4160.
11. Kunikowska J, Cieslak B, Gierej B, et al. [(68) Ga]Ga-prostate-specific membrane antigen PET/CT: a novel method for imaging patients with hepatocellular carcinoma. *Eur J Nucl Med Mol Imaging*. September 3, 2020 [In press].

12. Harris PA, Taylor R, Minor BL, et al. The REDCap consortium: Building an international community of software platform partners. *J Biomed Inform.* 2019;95:103208.
13. Harris PA, Taylor R, Thielke R, Payne J, Gonzalez N, Conde JG. Research electronic data capture (REDCap)--a metadata-driven methodology and workflow process for providing translational research informatics support. *J Biomed Inform.* 2009;42:377-381.
14. Fendler WP, Eiber M, Beheshti M, et al. 68Ga-PSMA PET/CT: Joint EANM and SNMMI procedure guideline for prostate cancer imaging: version 1.0. *Eur J Nucl Med Mol Imaging.* 2017;44:1014-1024.
15. Eiber M, Herrmann K, Calais J, et al. Prostate cancer molecular imaging standardized evaluation (PROMISE): proposed miTNM classification for the interpretation of PSMA-ligand PET/CT. *J Nucl Med.* 2018;59:469-478.
16. Fendler WP, Calais J, Eiber M, et al. Assessment of 68Ga-PSMA-11 PET accuracy in localizing recurrent prostate cancer: a prospective single-arm clinical trial. *JAMA Oncol.* 2019;5:856-863
17. Willatt J, Ruma JA, Azar SF, Dasika NL, Syed F. Imaging of hepatocellular carcinoma and image guided therapies - how we do it. *Cancer Imaging.* 2017;17:9.
18. Choi JY, Lee JM, Sirlin CB. CT and MR imaging diagnosis and staging of hepatocellular carcinoma: part I. Development, growth, and spread: key pathologic and imaging aspects. *Radiology.* 2014;272:635-654.
19. Amin MB, Edge S, Greene F, Byrd DR, Brookland RK, Washington MK, et al. *AJCC Cancer Staging Manual.* 8th ed. Springer International Publishing; 2017.
20. Lencioni R, Llovet JM. Modified RECIST (mRECIST) assessment for hepatocellular carcinoma. *Semin Liver Dis.* 2010;30:52-60.
21. Landis JR, Koch GG. The measurement of observer agreement for categorical data. *Biometrics.* 1977;33:159-174.
22. Clark T, Maximin S, Meier J, Pokharel S, Bhargava P. Hepatocellular carcinoma: review of epidemiology, screening, imaging diagnosis, response assessment, and treatment. *Curr Probl Diagn Radiol.* 2015;44:479-486.
23. European Association for the Study of the Liver. EASL clinical practice guidelines: management of hepatocellular carcinoma. *J Hepatol.* 2018;69:182-236.
24. Heimbach JK, Kulik LM, Finn RS, et al. AASLD guidelines for the treatment of hepatocellular carcinoma. *Hepatology.* 2018;67:358-380.

25. Verslype C, Rosmorduc O, Rougier P, Group EGW. Hepatocellular carcinoma: ESMO-ESDO clinical practice guidelines for diagnosis, treatment and follow-up. *Ann Oncol*. 2012;23 Suppl 7:vii41-48.
26. Boland P, Wu J. Systemic therapy for hepatocellular carcinoma: beyond sorafenib. *Chin Clin Oncol*. 2018;7:50.
27. Ingle PV, Samsudin SZ, Chan PQ, et al. Development and novel therapeutics in hepatocellular carcinoma: a review. *Ther Clin Risk Manag*. 2016;12:445-455.
28. Llovet JM, Ricci S, Mazzaferro V, et al. Sorafenib in advanced hepatocellular carcinoma. *N Engl J Med*. 2008;359:378-390.
29. Kudo M, Finn RS, Qin S, et al. Lenvatinib versus sorafenib in first-line treatment of patients with unresectable hepatocellular carcinoma: a randomised phase 3 non-inferiority trial. *Lancet*. 2018;391:1163-1173.
30. Cheng A-L, Kang Y-K, Chen Z, et al. Efficacy and safety of sorafenib in patients in the Asia-Pacific region with advanced hepatocellular carcinoma: a phase III randomised, double-blind, placebo-controlled trial. *Lancet Oncol*. 2009;10:25-34.
31. Li D, Sedano S, Allen R, Gong J, Cho M, Sharma S. Current treatment landscape for advanced hepatocellular carcinoma: patient outcomes and the impact on quality of life. *Cancers (Basel)*. 2019;11:841.
32. Mahalingam D, Peguero J, Cen P, et al. A phase II, multicenter, single-arm study of mipsagargin (G-202) as a second-line therapy following sorafenib for adult patients with progressive advanced hepatocellular carcinoma. *Cancers (Basel)*. 2019;11:83.
33. Roberts LR, Sirlin CB, Zaiem F, et al. Imaging for the diagnosis of hepatocellular carcinoma: A systematic review and meta-analysis. *Hepatology*. 2018;67:401-421.
34. Filippi L, Schillaci O, Bagni O. Recent advances in PET probes for hepatocellular carcinoma characterization. *Expert Rev Med Devices*. 2019;16:341-350.
35. Chalaye J, Costentin CE, Luciani A, et al. Positron emission tomography/computed tomography with 18F-fluorocholine improve tumor staging and treatment allocation in patients with hepatocellular carcinoma. *J Hepatol*. 2018;69:336-344.

FIGURES

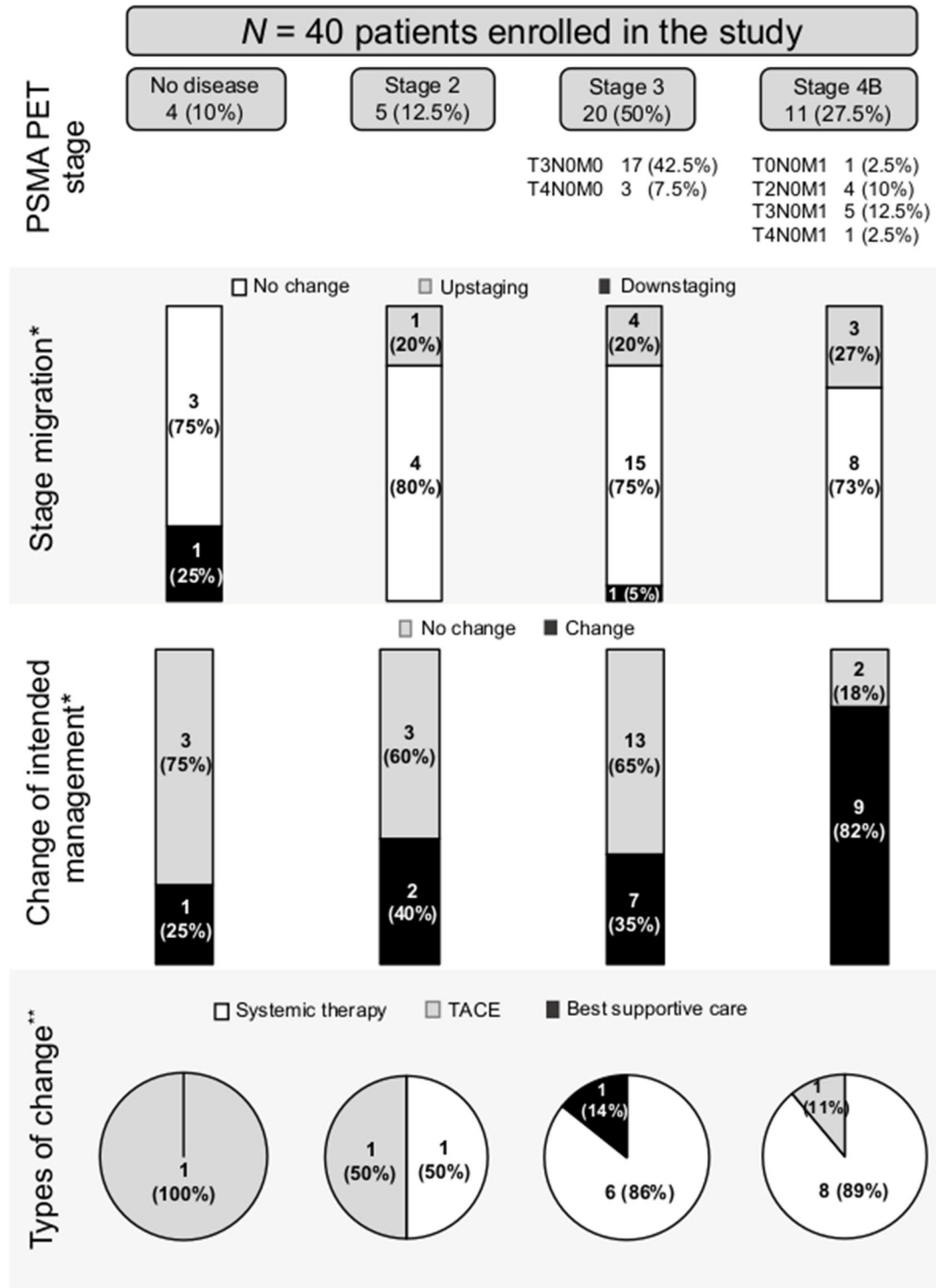


Figure 1. PSMA PET stage and change in management. (* % from PSMA PET stage; ** % from changed management)

TABLES

Table 1. Patient characteristics (N=40).

Variable	N (%) or median (range)
M:F ratio	5.7:1
Median age at diagnosis, years (range)	65 (37-81)
Primary diagnostic investigations, N (%)	
Histopathology	20 (50)
Imaging	31 (77.5)
AFP level	19 (47.5)
Comorbidities, N (%)	
Cirrhosis	28 (70)
Hepatitis B or C	18 (45)
Diabetes	11 (27.5)
NASH/steatosis	5 (12.5)
PVT or invasion	9 (22.5)
Ascites, N (%)	
None	29 (72.5)
Controlled	10 (25)
Refractory	1 (2.5)
Baseline investigations, median (range)	
BMI (kg/m ²)	27.4 (20.2-38.5)
AFP (ng/ml)	36.1 (1-19,078)
total bilirubin (µmol/liter)	0.8 (0.2-6.7)
albumin (g/l)	4.1 (2.6-5)
INR	1.1 (1-1.6)
ALKP (IU/l)	127 (33-937)
Child-Pugh Score, median (range)	5 (5-9)
Class A, N (%)	33 (82.5)
Class B, N (%)	7 (17.5)
Treatment received before PSMA PET/CT, N (%)	
None	27 (67.5)
Systemic treatment	2 (5)
Surgery	6 (15)
TACE or RFA	14 (35)
SIRT	4 (10)

AFP: alpha-fetoprotein; ALKP: alkaline phosphatase; BMI: body-mass index; INR: international normalized ratio; NASH: non-alcoholic steatohepatitis; PVT: portal vein thrombosis; RFA: radiofrequency ablation; SIRT: selective internal radiation therapy; TACE: transarterial chemoembolization.

Table 2. Accuracy, sensitivity, specificity, PPV and NPV between PSMA-PET and CT.

	Whole liver analysis		Right lobe (Segments 1, 4 – 8)		Left lobe (Segments 2,3)		Distant metastases	
	PSMA-PET	CT	PSMA-PET	CT	PSMA-PET	CT	PSMA-PET	CT
Accuracy (%)	97	97	97	94	86	91	100	94
Sensitivity (%)	97	97	97	94	77	85	100	67
Specificity (%)	100	100	100	100	91	95	100	100
PPV (%)	100	100	100	100	83	92	100	100
NPV (%)	80	80	83	67	87	91	100	93

Table 3. Comparison of staging between PSMA-PET and CT scans.

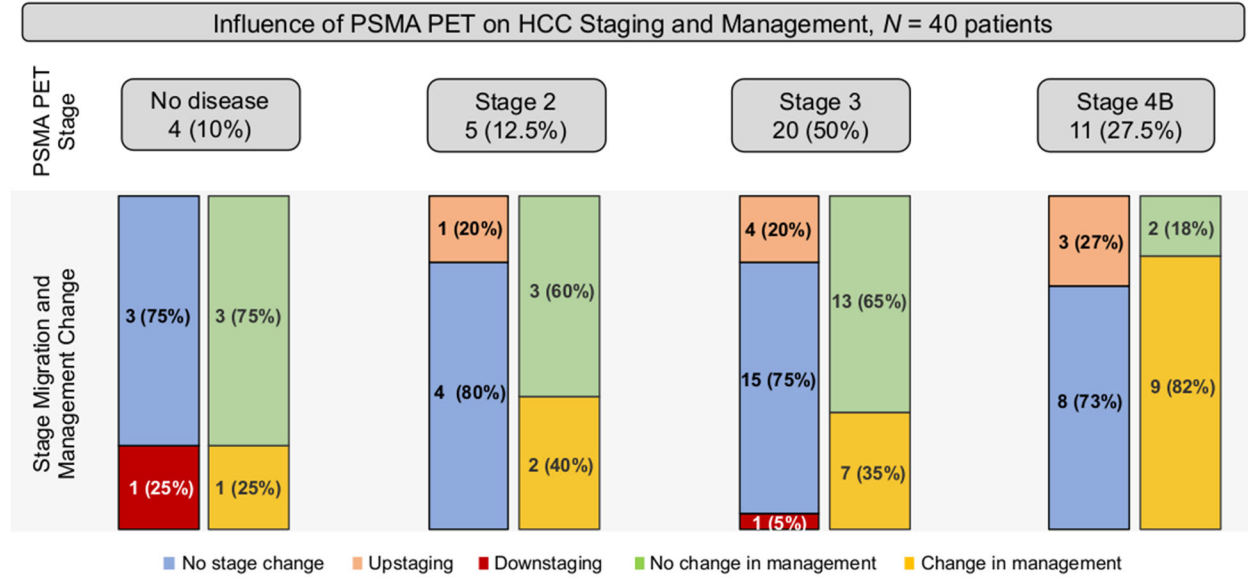
	PSMA-PET, N (%)	CT, N (%)
Stage 0 (T0N0M0)	4 (10)	4 (10)
Stage 2 (T2N0M0)	5 (12.5)	11 (27.5)
Stage 3	20 (50)	17 (42.5)
3A: T3N0M0	17 (42.5)	13 (32.5)
3B: T4N0M0	3 (7.5)	4 (10)
Stage 4B	11 (27.5)	8 (20)
T0N0M1 (bone)	1 (2.5)	-
T2N0M1	4 (10)	4 (10)
bone	2 (5)	1 (2.5)
mediastinal LN	1 (2.5)	2 (5)
mediastinal LN + bone	1 (2.5)	1 (2.5)
T3N0M1	5 (12.5)	2 (5)
bone	2 (5)	1 (2.5)
mediastinal LN	1 (2.5)	-
mediastinal LN + bone	1 (2.5)	-
cardiophrenic recess	1 (2.5)	1 (2.5)
T4N0M1 (bone)	1 (2.5)	2 (5)

Table 4: Stage migration through PSMA-PET and CT.

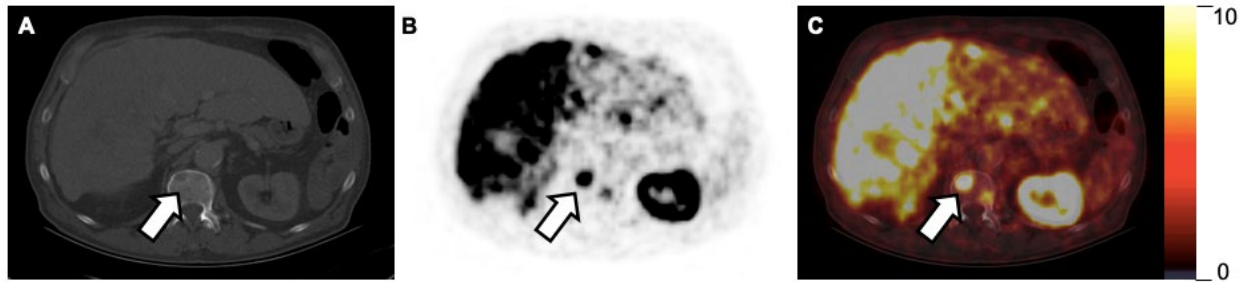
		PSMA-PET				
CT	Stage, N (%)	no disease	2	3A	3B	4B
		no disease	3 (7.5)	1 (2.5)*	0	0
	2	1 (2.5)**	4 (10)	4 (10)*	0	2 (5)*
	3A	0	0	12 (30)	0	1 (2.5)*
	3B	0	0	1 (2.5)**	3 (7.5)	0
	4B	0	0	0	0	8 (20)

*PET upstaging; **PET down-staging

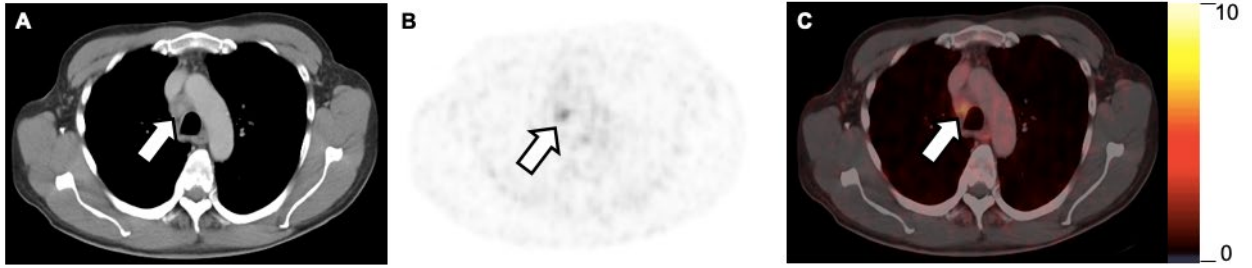
Graphical Abstract



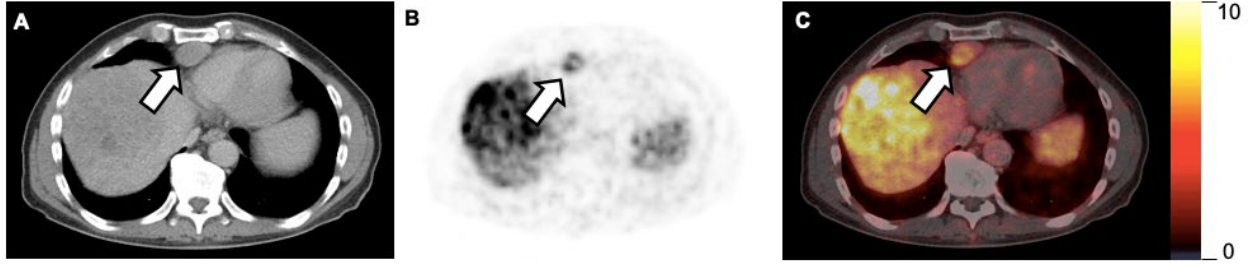
SUPPLEMENTAL FIGURES



Supplemental figure 1. (A) CT (B) PET and (C) fused ^{68}Ga -Ga-PSMA-11 PET/CT scan of a patient with disseminated bone metastases, confirmed by PET (high uptake with $\text{SUV}_{\text{max}} = 21.3$) and CT (long diameter 1.8 cm). The lesion here is seen in the lumbar vertebra (arrows).



Supplemental figure 2. (A) CT (B) PET and (C) fused ^{68}Ga -Ga-PSMA-11 PET/CT scan of a patient with mediastinal lymph nodes detected on both PET (intermediate uptake with $\text{SUV}_{\text{max}} = 4.4$) and CT (short diameter 1.9 cm), confirmed as positive by histopathology following lymph node dissection.



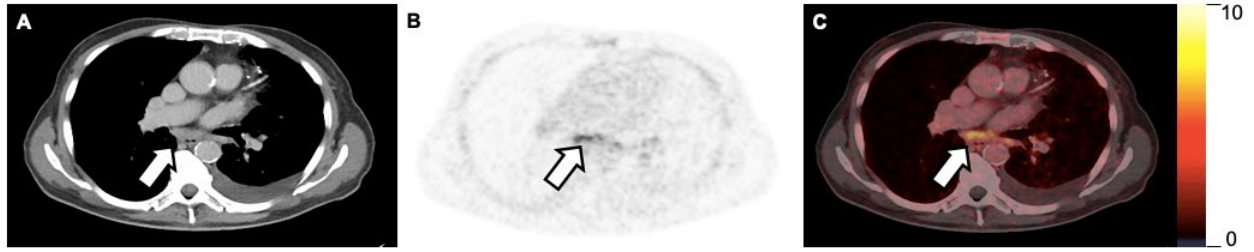
Supplemental figure 3. (A) CT (B) PET and (C) fused ^{68}Ga -Ga-PSMA-11 PET/CT scan of a patient with lymph nodes in the cardiophrenic angle, visible on both PET (intermediate uptake with $\text{SUV}_{\text{max}} = 7.2$) and CT (short diameter 2.6cm), confirmed on follow-up scans.



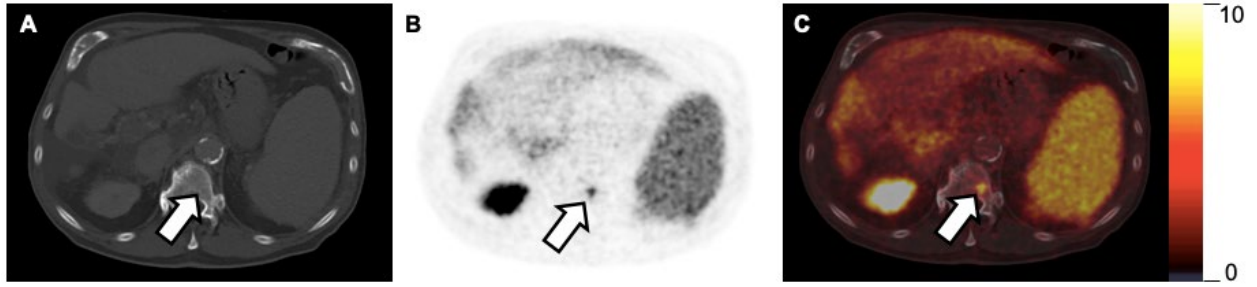
Supplemental figure 4. (A) CT (B) PET and (C) fused PET/CT of ^{68}Ga -Ga-PSMA-11 PET scan of a patient with distant osseous metastases in the right proximal femur, visible on PET with intermediate PSMA uptake ($\text{SUV}_{\text{max}} = 7.8$) and missed by CT, confirmed later on follow-up CT imaging.



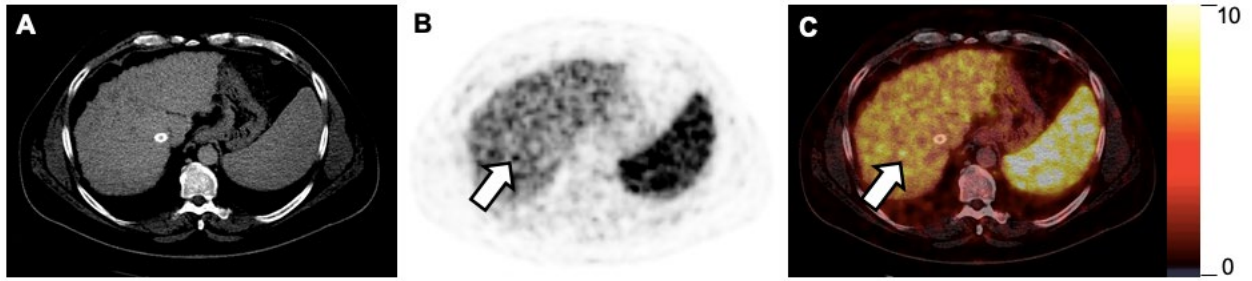
Supplemental figure 5. (A) CT (B) PET and (C) fused PET/CT of ^{68}Ga -Ga-PSMA-11 PET/CT scan of a patient with metastatic lesions in the right fourth rib seen on PET (intermediate PSMA uptake with $\text{SUV}_{\text{max}} = 5.4$), with non-specific findings on CT, as well as lesions in liver segments 4A/4B (not shown). Patient received localized treatment for liver and bone metastases, and follow-up scans confirmed resolution of all lesions.



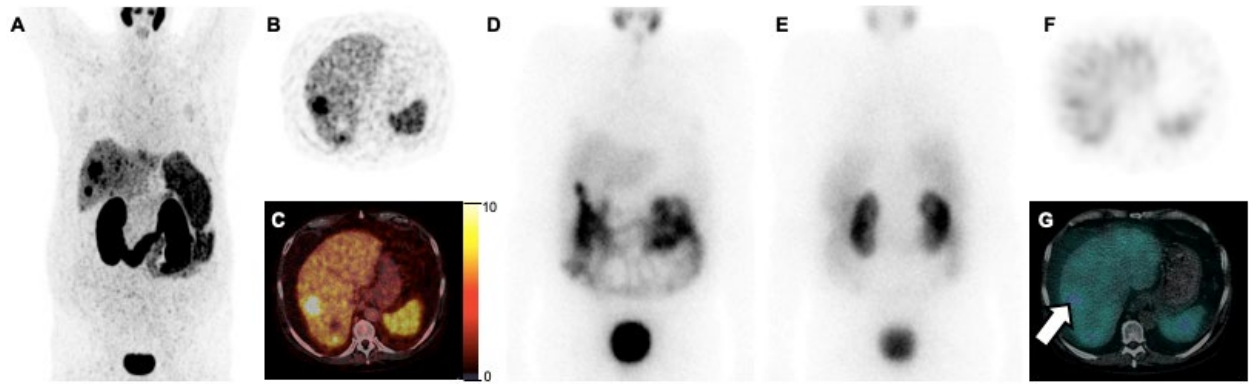
Supplemental figure 6-I (same patient in figure 6-II). (A) CT (B) PET and (C) fused PET/CT of ^{68}Ga -Ga-PSMA-11 PET/CT scan of a patient with metastatic lesions in mediastinal lymph nodes detected on PET (with intermediate PSMA uptake ($\text{SUV}_{\text{max}} = 5.4$), but not deemed pathological on CT (short diameter $<1\text{cm}$).



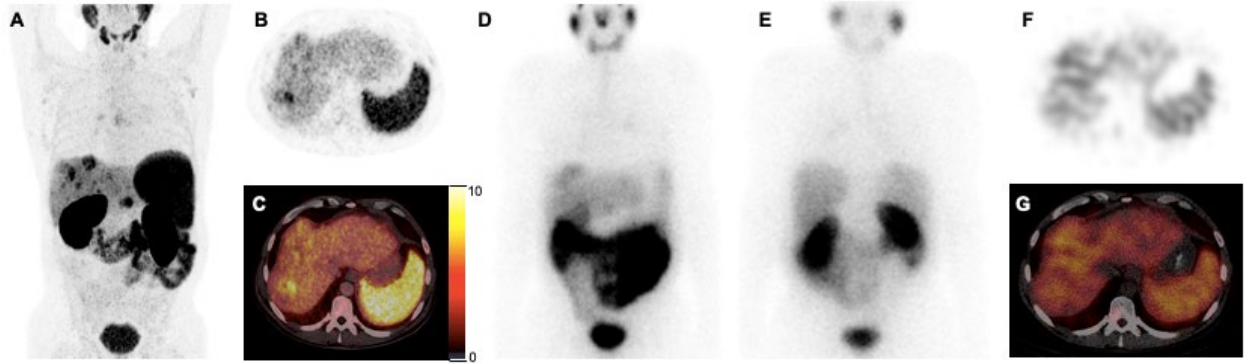
Supplemental figure 6-II (same patient in figure 6-I). (A) CT (B) PET and (C) fused PET/CT of ^{68}Ga -Ga-PSMA-11 PET/CT scan of a patient with metastatic lesions in the spine with intermediate PSMA uptake ($\text{SUV}_{\text{max}} = 7.3$), here seen in lumbar vertebra on PET but non-specific on CT.



Supplemental figure 7. (A) CT (B) PET and (C) fused ^{68}Ga -Ga-PSMA-11 PET/CT scan of a patient with mild PSMA uptake in liver segment V (intermediate uptake with $\text{SUV}_{\text{max}} = 4.9$) not visible on CT, and later confirmed by histopathology. The patient underwent TACE, and follow-up imaging confirmed complete resolution of the lesion.



Supplemental figure 8. (A) Maximum-intensity projection (B) PET and (C) Fused PET/CT of ^{68}Ga -Ga-PSMA-11 PET/CT scan for a patient before ^{177}Lu -Lu-PSMA-617 therapy, (D) Anterior and (E) Posterior views of planar whole body ^{177}Lu -Lu-PSMA-617 scintigraphy 1-day post therapy. 1-day post-therapy (F) SPECT and (G) Fused SPECT/CT revealed low accumulation of ^{177}Lu -Lu-PSMA-617 in the liver lesion (0.11 Gy/GBq, arrow). This patient had Child-Pugh class B HCC proven by histopathology and CT, in addition to cirrhosis and well-controlled ascites. Pre-imaging through bone scan, MRI and CT, as well as ^{68}Ga -Ga-PSMA-11 PET/CT performed all showed stage 2 disease with high PSMA expression ($\text{SUV}_{\text{max}} = 25$). The patient received one cycle of RLT with 5.9 GBq ^{177}Lu -Lu-PSMA-617 i.v. Given the low uptake of ^{177}Lu -Lu-PSMA-617 in tumor sites, therapy was discontinued. ^{177}Lu -Lu-PSMA-617 therapy was tolerated well with no adverse events noted. The patient subsequently underwent best supportive care.



Supplemental figure 9. (A) Maximum-intensity projection (B) PET and (C) Fused PET/CT of ^{68}Ga -Ga-PSMA-11 PET/CT scan for a patient before ^{177}Lu -Lu-PSMA-617 therapy, (D) Anterior and (E) Posterior views of planar whole body ^{177}Lu -Lu-PSMA-617 scintigraphy 1-day post therapy. 1-day post-therapy (F) SPECT and (G) Fused SPECT/CT revealed low accumulation of ^{177}Lu -Lu-PSMA-617 in the liver lesion (0.02 Gy/GBq). This patient also has Child-Pugh class B HCC proven by histopathology and CT, in addition to cirrhosis and hepatitis B. Pre-imaging as well as ^{68}Ga -Ga-PSMA-11 PET/CT revealed stage 3A disease limited to the liver, with high PSMA expression ($\text{SUV}_{\text{max}} = 11.1$). The patient received one cycle of RLT with 6.2 GBq ^{177}Lu -Lu-PSMA-617 i.v. Given the low uptake of ^{177}Lu -Lu-PSMA-617 in tumor sites, therapy was discontinued. ^{177}Lu -Lu-PSMA-617 therapy was tolerated well with no adverse events noted. The patient subsequently underwent best supportive care.

SUPPLEMENTAL TABLES

Supplemental table 1. Diagnosis of HCC lesions vs. dysplastic nodules on CT and MRI (1,2).

CT	MRI
Findings defined as HCC lesions	
Hyperenhanced nodule on arterial phase with washout relative to the liver parenchyma during the venous or delayed phases (3–5 min post injection)	
Capsular enhancement (persistent peripheral enhancing rim) seen on venous and delayed phases	
---	Lesion showing only arterial enhancement or only washout and pseudocapsule formation, if the lesion also demonstrates increased signal intensity on T2-weighted image, or if the lesion restricts diffusion
---	Intracellular lipid detected within a nodule on dual-echo in and opposed phase T1- weighted image
Findings defined as dysplastic nodules (i.e. not HCC lesions)	
Lesion with focal hepatic arterial enhancement, but without washout, capsule enhancement, or abnormally increased T2 signal	
Hyperattenuating lesion on unenhanced CT	Hyperintense lesion on T1-weighted images
Isoattenuating or hypoattenuating lesion in all phases (arterial, portal, and delayed)	Isointense or hypointense lesion on T2-weighted images

Supplemental table 2. Accuracy, sensitivity, specificity, PPV and NPV at the liver segment-level.

	Segment 1		Segment 2		Segment 3		Segment 4A		Segment 4B		Segment 5		Segment 6		Segment 7		Segment 8	
	PSMA PET	CT	PSMA PET	CT	PSMA PET	CT	PSMA PET	CT	PSMA PET	CT	PSMA PET	CT	PSMA PET	CT	PSMA PET	CT	PSMA PET	CT
Patients with detected lesions*	3	5	10	9	11	11	17	16	19	19	18	20	12	13	12	12	15	16
Accuracy	91.1%	91.1%	85.7%	94.3%	88.9%	94.4%	87.5%	87.1%	82.4%	82.4%	94.3%	88.6%	88.2%	73.5%	91.2%	82.9%	90.9%	85.3%
Sensitivity	50.0%	75.0%	72.7%	81.8%	81.8%	90.9%	93.3%	92.9%	93.3%	93.3%	90.0%	90.0%	75.0%	62.5%	80.0%	68.8%	83.3%	78.9%
Specificity	96.7%	93.3%	91.7%	100.0%	92.0%	96.0%	82.4%	82.4%	73.7%	73.7%	100.0%	86.7%	100.0%	83.3%	100.0%	94.7%	100.0%	93.3%
PPV	66.7%	60.0%	80.0%	100.0%	81.8%	90.9%	82.4%	81.3%	73.7%	73.7%	100.0%	90.0%	100.0%	76.9%	100.0%	91.7%	100.0%	93.8%
NPV	93.5%	96.6%	88.0%	92.3%	92.0%	96.0%	93.3%	93.3%	93.3%	93.3%	88.2%	86.7%	81.8%	71.4%	86.4%	78.3%	83.3%	77.8%

*Out of 36 patients with detectable disease.

NPV: negative predictive value; PPV: positive predictive value.

Supplemental table 3. Staging concordance between PSMA-PET and CT.

	CT findings, N (%)
PSMA-PET upstage to	8 (20)
stage 2	1 (2.5)
stage 3A	4 (10)
stage 4B (bone)	1 (2.5)
stage 4B (mediastinal lymph nodes)	1 (2.5)
stage 4B (bone and mediastinal lymph nodes)	1 (2.5)
PSMA-PET confirms staging of	30 (75)
no disease	3 (7.5)
stage 2	4 (10)
stage 3A	12 (30)
stage 3B	3 (7.5)
stage 4B (bone)	4 (10)
stage 4B (mediastinal lymph nodes)	2 (5)
stage 4B (bone and mediastinal lymph nodes)	1 (2.5)
stage 4B (cardiophrenic recess)	1 (2.5)
PSMA-PET downstage to	2 (5)
no disease	1 (2.5)
stage 3A	1 (2.5)

Suppl. table 4: Mean lesion size and SUV_{max} from a patient-based analysis.

PSMA-PET Stage	Liver		Extra-abdominal lymph nodes		Bone lesions	
	Mean lesion size in cm (range)	Mean SUV _{max} (range)	Mean lesion size in cm (range)	Mean SUV _{max} (range)	Mean lesion size in cm (range)	Mean SUV _{max} (range)
2	4.1 (2.5-6.2)	13.7 (9.2-25)				
3A	6.6 (3.1-10.8)	18.6 (7.6-55.4)				
3B	10.5 (7.1-16.5)	13.8 (12.9-14.4)				
4B	5.6 (1.4-11.1)	15.8 (9.5-30.4)	1.3 (0.5-2.6)	6.0 (4.4-12.3)	1.4 (0.4-2.6)	8.8 (2.9-21.3)
ALL	5.9 (0.6-16.5)	16.2 (5.9-55.4)				

Suppl. table 5: Post-PSMA-PET management changes.

Pre PSMA-PET	N (%)	Post PSMA-PET	N (%)	Change
		SIRT	15 (37.5)	No
SIRT	31 (77.5)	Systemic therapy	15 (37.5)	Yes
		TACE	1 (2.5)	Yes
Systemic treatment	2 (5)	Systemic therapy	1 (2.5)	No
		TACE	1 (2.5)	Yes
¹⁷⁷ Lu-Lu-PSMA-617 RLT	3 (7.5)	¹⁷⁷ Lu-Lu-PSMA-617 RLT	2 (5)	No
		Best supportive care	1 (2.5)	Yes
Active surveillance	3 (7.5)	Active surveillance	1 (2.5)	No
		TACE	1 (2.5)	Yes
		Disease ruled out	1 (2.5)	No
Best supportive care	1 (2.5)	Best supportive care	1 (2.5)	No

RLT: radioligand therapy; SIRT: selective internal radiation therapy; TACE: transarterial chemoembolization.

SUPPLEMENTAL REFERENCES

1. Willatt J, Ruma JA, Azar SF, Dasika NL, Syed F. Imaging of hepatocellular carcinoma and image guided therapies - how we do it. *Cancer Imaging*. 2017;17:9.
2. Choi JY, Lee JM, Sirlin CB. CT and MR imaging diagnosis and staging of hepatocellular carcinoma: part I. Development, growth, and spread: key pathologic and imaging aspects. *Radiology*. 2014;272:635-654.